

論文 / 著書情報
Article / Book Information

論題(和文)	
Title(English)	Optimal heliostat layout for concentrating solar tower systems
著者(和文)	宇多村 元昭, 玉浦 裕
Authors(English)	Motoaki Utamura, Yutaka Tamaura, Minoru Yuasa, Rina Kajita, Takashi Yamamoto
出典(和文)	, , ,
Citation(English)	Intn'l Conf. on Power Engn'g 07 (ICOPE2007), , ,
発行日 / Pub. date	2007, 10

Optimal Heliostat Layout for Concentrating Solar Tower Systems

Motoaki UTAMURA*, Tadahiko TAKAMATSU**, Minoru YUASA**, Rina KAJITA** and Takashi YAMAMOTO**

*Tokyo Institute of Technology, 2-12-1 Ookayama Meguro-ku Tokyo 152-8550 Japan
(E-mail: utamura@rccre.titech.ac.jp)

** Thermal Engineering & Development Co. Ltd.

3-18-14 Shin-Yokohama, Kouhoku-ku, Yokohama 222-0033 Japan

(E-mail: tad.takamatsu@ted-corp.co.jp)

Abstract: A methodology to give an optimal layout of a group of heliostats has been developed for concentrating solar tower systems. Given the maximum solar power together with optical parameters, the method determines an optimal configuration of a heliostat field around a tower where reflected beams are focused and a resultant annual solar energy collected. Various optical losses such as cosine factor, and an optical interference such as shadowing and blocking are taken into account in the calculation. Furthermore, spillage at a receiver collector is considered due to the spread of light that is derived from the effects of a finite solar disk and various errors inherent in optical hardware and control. It is found the spillage becomes significant at heliostats located in a distance from the tower farther than four times of tower height and dominates the configuration of the optimal heliostat layout.

Keywords: concentrating solar power, beam down system, heliostat field, spillage, shadowing, blocking, cosine factor

1. INTRODUCTION

Large scale solar thermal powers of mega-watt class have been commercialized in California USA as a parabolic trough system that utilizes two-dimensional solar concentration. To obtain higher concentration and a resultant higher thermal efficiency in power generation, a power tower system has been introduced which incorporates three-dimensional concentration as practiced in Solar one and two. The power tower system uses molten salt as heat transfer medium with thermal storage allowing 24 hour continuous operation of plant. For instance a 120MWt class commercial plant Solar Tres is ready to be erected in Spain. To seek a larger capacity beam-down optics has been investigated as shown in Fig.1[1].

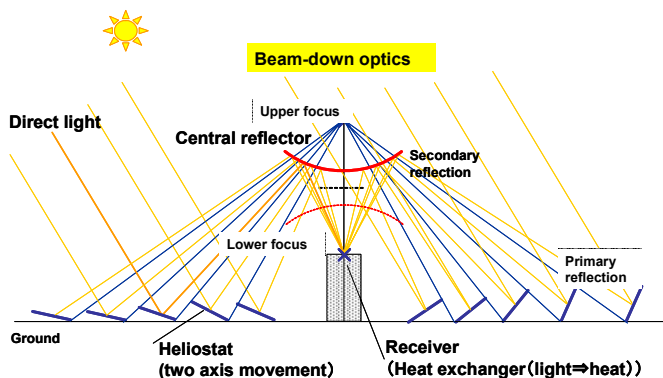


Fig.1 The concept of beam-down optics

The beam-down concept aims to redirect solar beam downward using an additional mirror, which enables heavy equipment such as heat exchanger to sit on the ground. Thus it principally fits a larger scale power than the tower top system. In order to realize this concept, however, there remain unresolved design issues. Several ideas are published to overcome the difficulties [2]. One of major issues is optics[3]. For example the solar beam experiences two reflections and a longer optical path to be finally absorbed in a receiver. Thus optics becomes complex and requires more reliable analysis tool of optics to provide accurate prediction of its performance. Half of the total equipment cost of the power tower system comes from that of heliostats. Therefore optimization of heliostat layout is crucially important design issue leading to reduction of power generation cost. There were substantial

works in the past[4] but assume no beam down system. This paper describes the methodology to optimize layout for a group of heliostats in beam-down central receiver optics and aims to identify the effects of optical parameters to affect optical performance.

2. OPTIMAL HELIOSTAT LAYOUT PROBLEM

2.1 Beam-down optics

Beam-down optics consists of heliostat field, a central reflector and a receiver. The heliostat field consists of a group of mirrors placed on the earth having two-axis movement to reflect the direct light from the sun always to the upper focus of the central reflector regardless of the sun movement. The central reflector is a monolithic or pieces of hyperboloid that redirects the reflected rays from the heliostats to the lower focal point where the center of the aperture of the receiver is located. Thus, the sun light is first reflected by a heliostat (primary reflection), redirected by a central reflector (secondary reflection) and finally captured at the receiver placed near the ground to be converted to heat. The amount of solar energy per a heliostat is larger in the area north to a tower where the central reflector is installed in the north hemisphere while optical interferences among adjacent heliostats are also significant. They affect reduction of an effective area of mirrors. Therefore there exists a design issue of an optimal heliostat layout i.e. the problem to solve the heliostat layout that meets annual energy demand with minimum number of heliostats.

2.2 Influencing parameters

There are two causes to dominate the amount of energy absorbed in the receiver: that is 1) reduction of effective heliostat mirror area and 2) induction of spillage of beams out of the receiver. The parameters associated with 1) are ① inclination of heliostat, what is called cosine effect, and ② optical interferences caused by shadowing and blocking (S&B). The former is the difference in the direction between the vector outward normal to the heliostat mirror surface and the vector pointing the sun. The latter is that the shadowing prevents sun light of coming in the heliostat mirror and the blocking does reflected one of passing through. On the other hand, as for 2) there are ③ effects of finite solar disk angle and plane nature of heliostat facet, and ④ deviation from design values in manufacturing, installation and delay in

control the movement of a heliostat. In the present analyses, optimal layout was discussed in two steps. The first step treats the problem without spillage, i.e. only the cause 1) and the second step with spillage, i.e. causes 1) and 2) at the same time respectively.

3. OPTIMAL LAYOUT WITHOUT SPILLAGE

3.1 Required field area (the theoretical lower limit value)

Let us consider the problem to obtain the layout to avoid S&B effect and yield a minimum field area to a given annual energy. Prior to this concentrating energy density Theoretical lower limit value was obtained by use of continuum model in which infinitesimally small heliostat is considered.

(1) Power density per heliostat

Solar power received by unit heliostat mirror area normalized by DNI(Direct normal insolation) s is $s = \mathbf{e}_1 \cdot \mathbf{n} = \mathbf{e}_2 \cdot \mathbf{n}$ and the length of shadow SL and the length of blocking BL are $SL = s/e_{1z}$, $BL = s/e_{2z}$ respectively. Here, \mathbf{e}_1 , \mathbf{e}_2 , \mathbf{n} are unit vectors of pointing the sun, pointing the upper focus and outward normal to the mirror surface of the heliostat respectively. Theoretical upper limit of number density of heliostat per unit field area m is expressed by $1/\max(SL, BL)$ and power collected by heliostats within unit field area ρ is

$$\rho = s \cdot m = \min(e_{1z}, e_{2z}).$$

$$\rho = \min(e_{1z}, e_{2z}) \quad (1)$$

Eq.(1) is a function of radial distance to the origin of the field where central reflector is located and the time. Hence, the spatial distribution of ρ is of symmetry around the origin whichever ρ may represent either power or energy.

(2) Annual energy density per heliostat

Average number density over the year \bar{m} may be defined as weighted by annual insolation.

$$\bar{m} = \frac{\sum (m \times \tau_{atm} \times s)}{\sum (\tau_{atm} \times s)}, \quad (2)$$

where τ_{atm} is the attenuation factor of direct light due to atmosphere and a function of sun altitude. \sum approximates time integration over a year. Using this, annual energy collected by a heliostat on a calculation grid (i, j) is

$$A_{ij} = \int \rho dt / \bar{m} \quad (3)$$

$A_{i,j}$ implies the ratio of actual energy collected by a unit area heliostat to those collected by a unit area plane facing the sun all the way, i.e. DNI. Fig.2 shows the contour of $A_{i,j}$ at the altitude of 37deg in north hemisphere with upper focus as high as 62m. North direction is axis upward, the unit of length is meter. The maximum value was 0.944 located in the north neighborhood of the origin of coordinates. Using this minimum possible field as well as area of heliostat mirrors necessary to attain the required power can be obtained. That is, the area of heliostat mirrors can be calculated by $\sum_{(i,j)} A_{i,j} \Delta x \Delta y$ by selecting the grid (i, j) one by one in

a manner such as

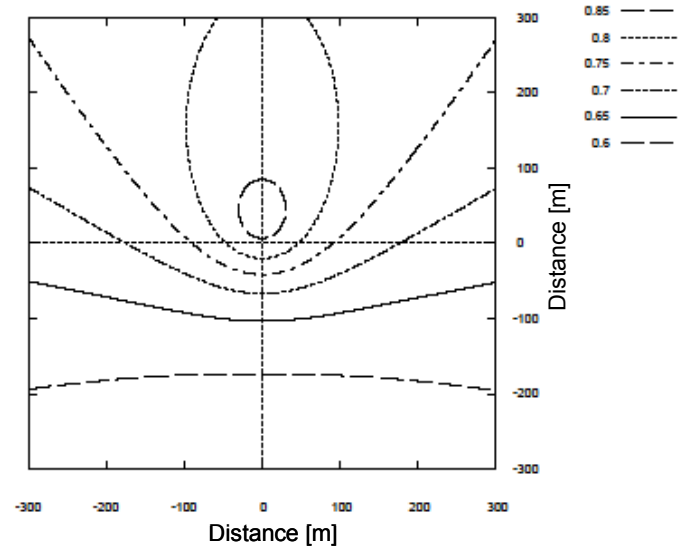


Fig.2 Contour of $A_{i,j}$

from the largest $A_{i,j}$ in order until it reaches the required energy. Otherwise it is possible to obtain a mirror area to realize a given power at a specific time (say, at noon of summer solstice) that maximizes annual energy. To do this, one has only to calculate power at each node (i, j) in addition to $A_{i,j}$. Then to select nodes one by one in the manner same as above until required power is reached. In this case annual energy can be obtained at the same time. Fig.3 shows the result with a power of 22.6MWt at noon of summer solstice. Finite size quadrilateral heliostat has a dimension of 6.8m (width)*4.9m (height) composed of 35 square facets. Calculation assumed movement of heliostat mirror was controlled facet by facet.

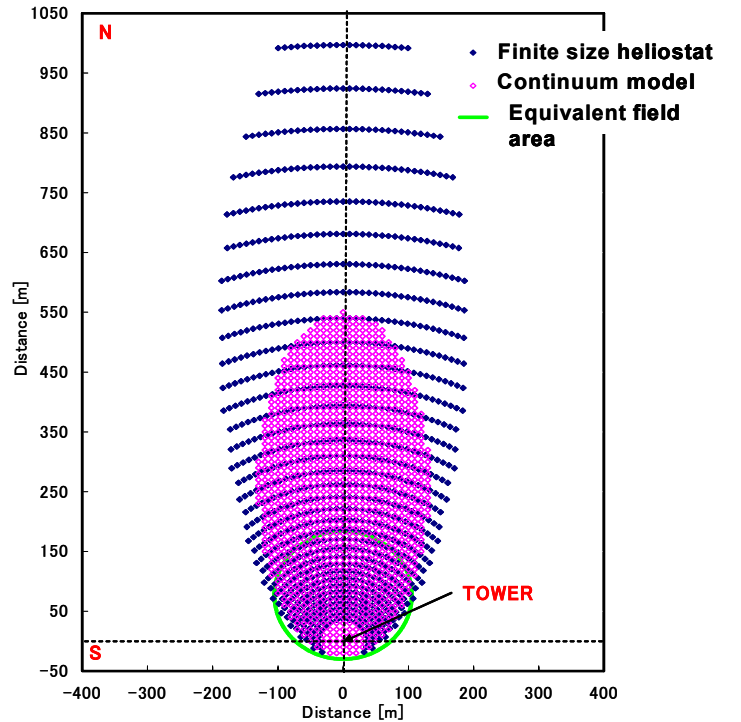


Fig.3 Optimal heliostat layout without spillage effect

As was expected from Fig.2 the optimal heliostat field resulting from continuum model, an ideal model thereafter, has an oval shape prolonged to the north with the tower present toward the south end of the oval. It is seen far more field area is required than an equivalent insolation on the ground denoted by a circle. This is due to a distance between heliostats required to avoid blocking. Algorithm to allocate finite size heliostats over the field is as follows:

- (1) Draw concentric circles around the tower with increment in radius determined by $\max(SL_r, BL_r)$ where suffix r denotes radial component of length.
- (2) Calculate $\max(SL_c, BL_c)$ where suffix c denotes circumferential component of length at an intersection between each circle and straight line directed to north and passing the origin.
- (3) Prepare possible seats on a circle with a pitch of $\sim \max(SL_c, BL_c)$
- (4) Physical properties at a seat were interpolated from those at grids surrounding the seat
- (5) Also distance between adjacent heliostats to avoid mechanical interaction was considered.

Optimized heliostat field using finite heliostat requires even more field area than the ideal layout. It is because in order to avoid blocking more field area unavailable was needed than that of ideal layout by continuum model. The number of heliostats required in continuum model was 1015 whilst the equivalent number was 1069 to give the same power.

3.2 Field shape to maximize power

Let us compare optimized shapes of ideal heliostat field between annual energy based and instant power based. Computational domain was selected from -100m to 1000m in south- north direction. Figs.4 and 5 show power based heliostat field shapes with 20.0MWt at noon on the summer and winter solstices. Each shape resulted from minimum number of heliostats to meet the specified power among possible layouts. The annual energy based shape by continuum model depicted in Fig.3 is considered reasonable because it looks averaged between two power based shapes in Figs.4 and 5.

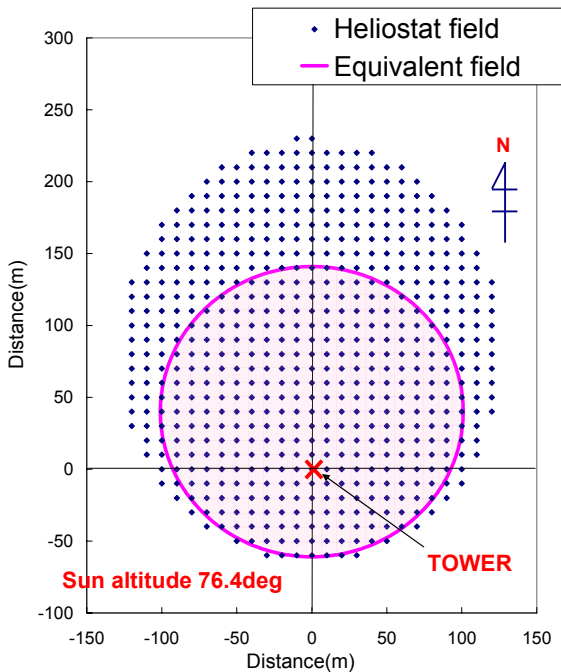


Fig.4 Optimal shape of heliostat layout based on power at noon of the summer solstice

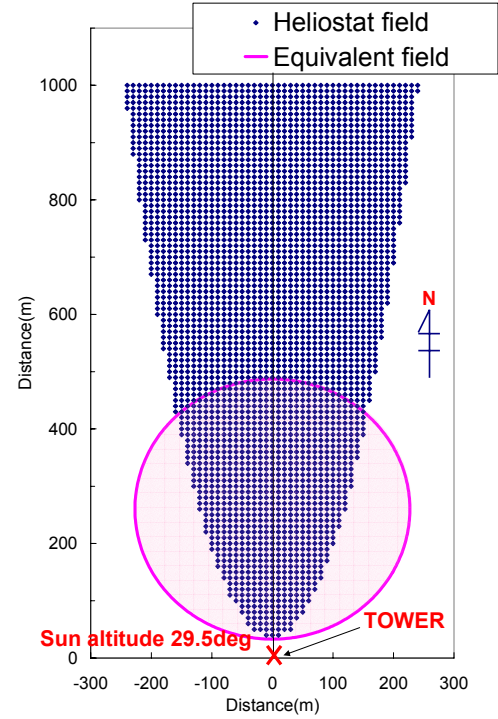


Fig.5 Optimal shape of heliostat layout based on power at noon of the winter solstice

3.3 Effect of altitude

Effect of altitude on the layout is shown in Fig.6 with the same number of heliostats 400. Two altitudes 47deg and 37deg gave powers 8.9MW and 9.7MW respectively. In terms of annual energy based optimization sensitivity of altitude was found small.

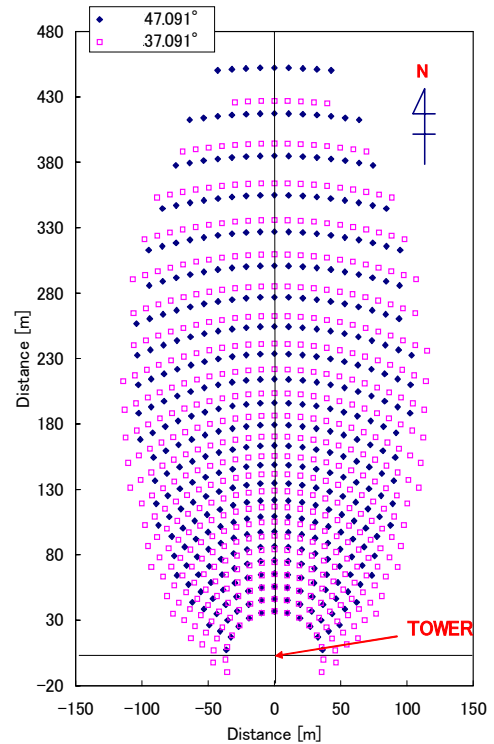


Fig.6 Effect of altitude

4. OPTIMAL LAYOUT WITH SPILLAGE

4.1 Method of analysis

In the preceding chapter the amount of solar energy or power captured by a group of heliostats was considered and optimal layout of heliostat field was obtained that gives minimum number of heliostats and their locations to achieve a specified solar energy or a power. In this chapter, the amount of solar energy captured by a receiver is considered in which spillage of reflected beams or incoming beams will be taken into account to optimize heliostat field layout. Optical simulator using Ray Tracing method coupled with Monte Carlo method [5] was used to accommodate calculation of the dilution of concentrating solar beams. Standard optical geometry adopted here is shown in Fig.7. Tracking the sun was assumed to be controlled facet by facet in the calculation. In this calculation solar disk was discretized. Reflected ray at heliostat and central reflector was treated in a stochastic manner and deviated from right angle with given angles as standard deviations.

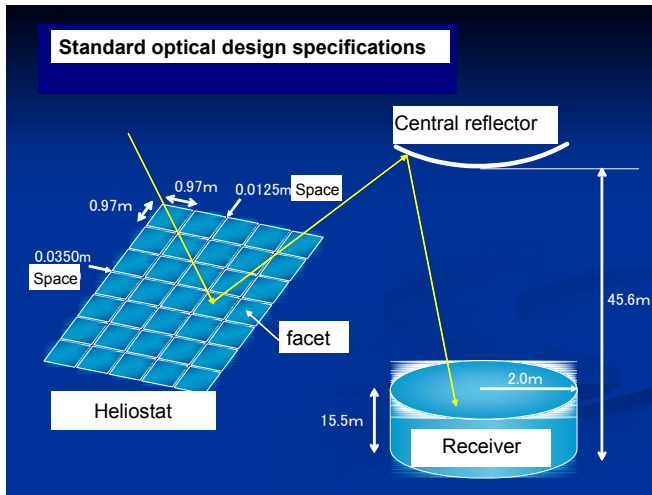


Fig.7 Standard optical configuration

4.2 Results

Fig.8 shows an example of flux distribution on the aperture plane of the receiver. The aperture of 4m in diameter whose edge is shown by a circle was assumed in the calculation to determine heliostat field layout. Spillage means rays dropped out of the circle. The diameter significantly affects the optimized shape of the heliostat field.

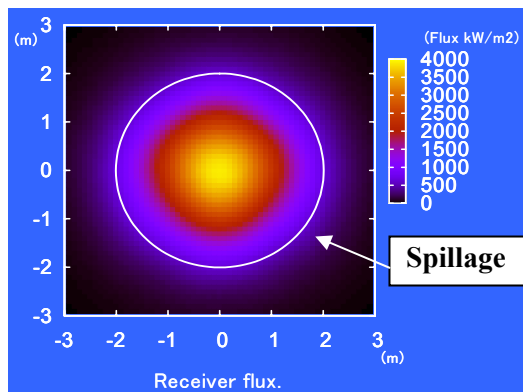


Fig. 8 Flux distribution on the aperture plane of receiver

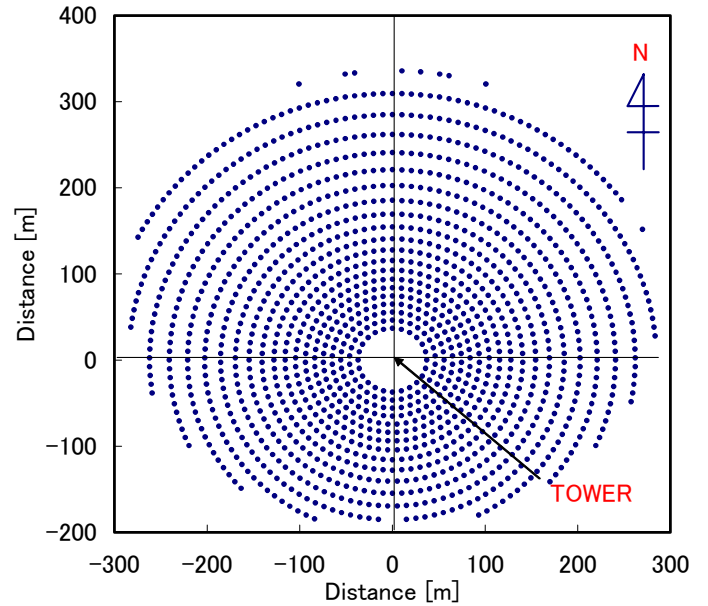


Fig.9 Optimized heliostat field layout with spillage considered

Fig.9 shows optimized heliostat field layout with spillage considered to maximize annual energy under the condition of the power of 22.6MW at summer solstice. Optimized shape is drastically changed from that based on the amount of energy captured at heliostats. Almost circle instead of oval shape was obtained as optimum shape. The number of heliostats required was 1456. This indicates the significance of the effect of spillage.

Diffusion of flux depends on the optical path length from heliostat to the receiver via. central reflector. Hence the effect of the distance on the amount of spillage was investigated. Fig.10 shows the result. The range of power at the same distance shows variation of power on the circumference of the circle. From this result it is shown beyond 250m apart north to the central reflector no seat exists that exceeds the energy captured at heliostat. This means no allocation of heliostat without spillage exists beyond the distance more than four times of upper focus height. Considering this observation and the Fig.10 one could find a bit larger aperture diameter could enhance optical performance.

Upper focus height: 61 m

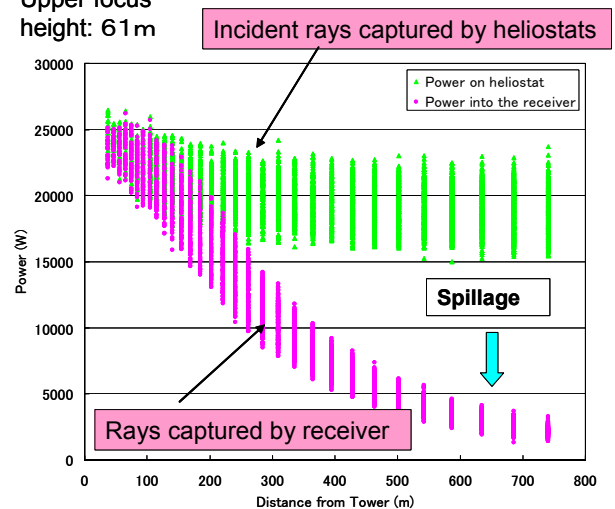


Fig.10 Effect of location of heliostat on spillage

4.3 Effect of optical uncertainties

Table 1 shows input data for angle uncertainties in terms of standard deviation and calculated radius at receiver aperture to each stochastic process. In this case the diameter of receiver aperture was 6m. Calculated radius is a measure of the amount of spillage. Those of solar disk and facet geometry were obtained from Monte Carlo calculations. Those two factors are seen to dominate the extent of diffusion of concentrating flux and induce resultant spillage from receiver. The effect of unevenness of the mirror facet of the central reflector on the spillage is small because of a shorter distance from there to the receiver.

Table 1 Standard deviations

	Stochastic processes	$\sigma(\text{mrad})$	$\sigma(\text{m})$
(1)	Solar disk	4.654mrad	1.6
(2)	Unevenness of heliostat	1.734mrad	0.79
(3)	Installation error	1.025mrad	0.46
(4)	Tracking error		
(5)	Unevenness of central Reflector	1.734mrad	0.08
(6)	Facet geometry	-	2.57
Total		-	3.21

Fig.11 shows effect of optical error in heliostat unevenness on energy collected at receiver. It is seen the spillage becomes significant beyond 2mrad(0.002rad).

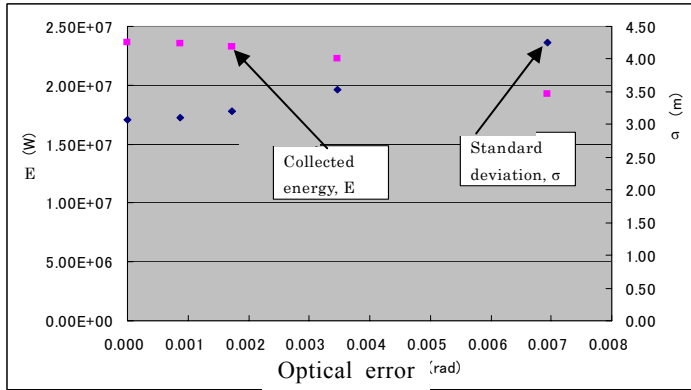


Fig.11 Effect of heliostat optical error on energy collected at receiver

Fig.12 shows optical losses relative to DNI. Cosine effect, and a product of S & B and reflection loss at heliostat contributes to optical loss by 30.8% and 10.5% respectively. Shadow of central reflector over the heliostats reduces energy by 7.9% and spillage out of receiver aperture is 4.0%. Heliostat incident energy was 12.3% of the energy received by the area of the envelope of heliostat field. Hence, $12.3 \times 42.4 / 69.2 = 7.5\%$ of solar energy on the heliostat field was estimated to be transferred to heat at receiver. Also, $1.8\% + 7.9\% = 9.7\%$ is additional optical loss due to beam down system over tower top system.

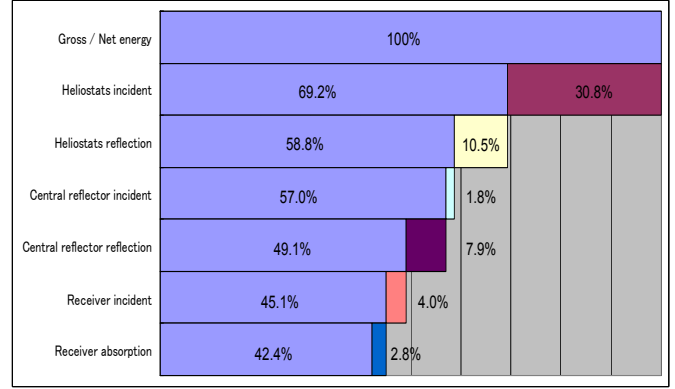


Fig.12 Contents of optical losses

5. CONCLUSIONS

A methodology to generate an optimal heliostat layout to maximize annual solar energy received by a beam down central receiver system was developed. Using continuum optical model annual energy received by a heliostat and its number density without optical interference (shadowing and blocking) was derived at computational grids in the heliostat field. Based on this knowledge coordinates for heliostats to be located were generated that minimize optical interference with heliostats in the neighborhood. Using Monte-Carlo ray tracing optical simulator newly developed minimum number of heliostats were selected to give a required annual energy received by the receiver. In the calculation spillage out of the receiver was taken into consideration. Resultant envelope shape of heliostat field was close to a circle due to the effect of spillage very different from that calculated without spillage effect. In the present beam down configuration it was found spillage becomes significant for heliostats located four times farther than the tower height. Among uncertainties those associated with facet mirror geometry (size and curvature) was found most significant in the standard optical design specifications adopted here.

6. UNITS AND SYMBOLS

6.1 Units

- A_{ij} ratio of annual energy collected by a unit area heliostat at to that on a unit area plane always facing direct to the sun at the field position (i,j) (=Eq.(3))
- BL blocking length (m)
- \mathbf{e}_1 unit vector pointing the sun (-)
- \mathbf{e}_2 unit vector pointing the upper focus of the central reflector (-)
- m heliostat number density ($1/\text{m}^2$)
- \mathbf{n} unit vector outward normal to the mirror surface of the heliostat (-)
- SL shadowing length (m)
- s solar power received by a heliostat with unit mirror area ($1/\text{m}^2$)
- Δx computational mesh in the east-west direction (m)
- Δy computational mesh in the south-north direction (m)

Greek

- ρ solar power collected by heliostats within unit field area (W/m^2)
- τ_{atm} atmospheric attenuation of the sun light (-)

Suffices

z vertical component of a vector

r radial direction

c circumferential direction

1z Z-component of the unit vector \mathbf{e}_1

2z Z-component of the unit vector \mathbf{e}_2

6.2 Symbols

DNI Direct normal insolation (W/m^2) or ($\text{J/m}^2/\text{year}$)

REFERENCES

- [1] Hasuike, H. Yoshizawa, Y., Suzuki, A. and Tamaura, Y., “Study on design of molten salt solar receivers for beam-down solar concentrator”, *Solar energy*, 80, pp. 1255-1262, 2006
- [2] Tamaura, Y. et al., “Solar heat collector, sunlight collecting reflector, sunlight collecting system and solar energy utilization system”, *WO2006/025449 A1*; 2005
- [3] A. Segal and M. Epstein; The Optics of the Solar Tower Reflector”, *Solar Energy*, Vol. 69, Nos. 1-6, pp. 229-241, 2001
- [4] Sanches, M. and Romero, M., “Methodology for generation of heliostat field layout in central receiver systems based on yearly normalized energy surfaces”, *Solar Energy*, Vol. 80, pp. 861-874, 2006
- [5] Utamura, M., et al., “Development of Optical Simulator for Solar Thermal Concentrating System (in Japanese)” *Proc. Solar Energy Conference*, 2006.